Pythagorean coupling: Complete population transfer in a four-state system

Haim Suchowski,[1,3,*] Yaron Silberberg,[1,†] and Dmitry B. Uskov[2,3,‡]

[1]*Department of Physics of Complex Systems, Weizmann Institute of Science, Rehovot IL-76100, Israel*
[2]*Department of Physics and Engineering Physics, Tulane University, New Orleans, Louisiana 70118, USA, and Brescia University,*
Division of Mathematics and Natural Sciences, Owensboro, Kentucky 42301, USA
[3]*Kavli Institute for Theoretical Physics, Santa Barbara, California 93106, USA*

Complete population transfer in a four-coupled-modes system is analyzed from a geometrical point of view. An analytical solution of the dynamics is written by the use of two distinct frequencies, the generalization of the single Rabi frequency of the two-state dynamics. We also present its visualization on two separate Bloch spheres with two independent torque equations. With this scheme we analytically derive the requirements for complete population transfer in a four-state quantum system. Interestingly, the solutions are found to be linked to fundamental number theory, whereas complete population transfer occurs only if the ratios between coupling coefficients exactly match a set of Pythagorean triples.

Complete population transfer from one state to another is a subject of extensive research for a variety of classical and quantum systems. Coherent manipulation of population of states in atomic and molecular quantum systems [1–3], spin control in nuclear magnetic resonances [4], quantum information processing [5,6], and directional optical waveguide technology [7] are only a few examples where complete population transfer between states is desired.

In general, solutions of time-dependent dynamical coupled equations are difficult to obtain analytically, and even for the simplest case of a two-state coupled system, realized by a spin-$\frac{1}{2}$ particle or a two-state atomic system, only a handful of analytical solutions is known. For example, in the well-known solution for a two-state system with a constant coupling field [1], complete population transfer between two orthogonal states occurs only when the frequency of an external driving field is on resonance with the energy difference between the states and only at discrete times, known as Rabi flopping times, which is inversely proportional to the strength of coupling.

The task of finding schemes for complete population transfer between selected states becomes increasingly difficult in multistate coupled systems. Group-theoretical methods offer a rigorous tool of how to determine whether a system is *wave function controllable*, i.e., whether any initial state in the system can be transferred into an arbitrary final state [8,9]. However, these methods are nonconstructive and do not provide a general recipe for implementing a complete population-transfer scheme for a concrete system. So far, there are only a limited number of systematic methods which can provide this goal. Among them are the schemes exploiting adiabatic evolution, which achieve this goal asymptotically, with the requirement of strong pairwise sequence of coupling pulses [2,10–13]. Also, few solutions for the general N-state systems can be found. Those require special relations of their coupling coefficients. A known example of such solutions is the spin-group system, which is the incorporation of the su(2) dynamics in an N-level system [14,15].

This research explores the dynamics of four-coupled-mode equations and the constraints for achieving complete population transfer between two nonadjacent states. Contrary to previous research of such systems, we explore its dynamics from a geometrical point of view. For the two-state system, the geometrical visualization on the Bloch sphere plays an important role in developing a clear, intuitive understanding of the two-state dynamics [16,17]. The approach which is developed here helps to extend the geometric representation of two-level dynamics into four-state systems. These systems are of particular importance for quantum information processing technology, where two-qubit quantum logic gates serve as elementary building blocks for designing fully functional scalable devices [5,18,19]. The analysis is based on a known equivalence from continuous group theory — the isomorphism between the the four-dimensional orthonormal group, which is the rotation of vector in four dimensions, known also as SO(4), and two separate two dimensional spacial unitary groups, each exhibiting dynamical symmetry of SU(2). We show that the evolution can be viewed on two different Bloch spheres, each with its unique Rabi frequency and effective detuning.

When the requirements of obtaining complete population transfer in a four-state system are analyzed, we find that those impose certain analytical relations on the coupling coefficients, which are surprisingly connected to families of Pythagorean triples. We show that these relations are identical to the equation for all primitive Pythagorean triples (PPTs), which is a set of three integer numbers a, b, and c, which does not possess a common factor and satisfies the equation $a^2 + b^2 = c^2$. In this article, several aspects of such solutions in the context of atomic physics are presented and discussed. We note that our analytical treatment can be implemented to other physical realizations as well.

The article is organized as follows: In Sec. I we show the decomposition of a four-state dynamics into two independent qubits. In the analysis we discuss two frames, the Lab frame and the Bell frame, which are important bases for the analytical and geometric analysis. Section II presents the analytical

‾‾‾‾‾‾‾‾
*haim.suchowski@weizmann.ac.il
†yaron.silberberg@weizmann.ac.il
‡uskov@tulane.edu

solution of such dynamics and its geometrical interpretation on two Bloch spheres. Section III deals with the special case of nearest-neighbors coupling of the four-state dynamics. The similarity with the two-mode dynamics is discussed. Section IV presents the Pythagorean inversion scheme and its unique properties. We also give a protocol to generate such symmetries and show the effects of variation of the parameters that control the dynamics.

I. DECOMPOSITION OF A FOUR-STATE DYNAMICS INTO TWO INDEPENDENT QUBITS

Let us start by writing the evolution of a four-dimensional wave function using the Schrödinger equation,

$$\frac{\partial \rho}{\partial t} = -iH\rho, \qquad (1)$$

where, $\rho(t) = [a_1(t), a_2(t), a_3(t), a_4(t)]$, with $a_n(t)$ as the probability amplitude of each state and $\hat{H}$ is the following Hamiltonian:

$$\hat{H} = \begin{pmatrix} 0 & V_{12} & -iV_{13} & V_{14} \\ V_{12} & 0 & V_{23} & -iV_{24} \\ iV_{13} & V_{23} & 0 & V_{34} \\ V_{14} & iV_{24} & V_{34} & 0 \end{pmatrix}. \qquad (2)$$

Here V_{ij} represents general coupling coefficients between the states, which are real valued. In the following treatment we consider a laser-field-driven four-level atom as an example of a physical realization of such systems. In this context, after considering the rotating wave approximation, the coupling coefficients are $V_{ij} = \mu_{ij}\epsilon(t)/\hbar$. Here $\epsilon(t)$ is the field amplitude and μ_{ij} are dipole matrix elements between levels i and j. This basis is noted as the Lab frame. A unique case of the system is the case of periodic nearest-neighbor couplings with $V_{13} = V_{24} = 0$, which is the diamond-type four-level structure that appears in many physical systems. If also $V_{14} = 0$, a ladder-type system is obtained.

An important feature of this problem is that it is solvable using geometric tools of su(2) rotations. This Hamiltonian can be separated into two distinct subsymmetries of su(2) and can be viewed as an element of su(2) ⊕ su(2) Lie algebra (explicit algebraic decomposition is shown in the Appendix):

$$\hat{H} = \frac{(V_{12} + V_{34})}{2}\hat{I}^{(1)} \otimes \hat{\sigma}_x^{(2)} + \frac{(V_{23} + V_{14})}{2}\hat{\sigma}_x^{(1)} \otimes \hat{\sigma}_x^{(2)}$$
$$+ \frac{(V_{12} - V_{34})}{2}\hat{\sigma}_z^{(1)} \otimes \hat{\sigma}_x^{(2)} + \frac{(V_{23} - V_{14})}{2}\hat{\sigma}_y^{(1)} \otimes \hat{\sigma}_y^{(2)}$$
$$+ \frac{(V_{13} + V_{24})}{2}\hat{\sigma}_y^{(1)} \otimes I^{(2)} + \frac{(V_{13} - V_{24})}{2}\hat{\sigma}_y^{(1)} \otimes \hat{\sigma}_z^{(2)}, \qquad (3)$$

where we used the known Pauli matrices

$$\hat{\sigma}_x = \begin{pmatrix} 0 & 1 \\ 1 & 0 \end{pmatrix}, \quad \hat{\sigma}_y = \begin{pmatrix} 0 & -i \\ i & 0 \end{pmatrix}, \quad \hat{\sigma}_z = \begin{pmatrix} 1 & 0 \\ 0 & -1 \end{pmatrix}, \qquad (4)$$

with an upper index (1) and (2) associated with qubits 1 and 2, indicating inner or outer SU(2) symmetry, respectively. The following decomposition is best seen in the Bell frame, which

is obtained by performing a similarity transformation using the known Bell (unitary) matrix:

$$\hat{W} = \frac{1}{\sqrt{2}} \begin{pmatrix} 1 & 0 & 0 & 1 \\ 0 & 1 & 1 & 0 \\ 0 & 1 & -1 & 0 \\ 1 & 0 & 0 & -1 \end{pmatrix}. \qquad (5)$$

The new wave functions will then become a superposition of the original wave functions $|\psi_n^B\rangle = W|\psi_n\rangle$, where we denoted $|\psi_n^B\rangle$ as the new Bell wave functions. In the Bell basis, two distinct su(2) subalgebras can be clearly identified

$$\hat{H}_B = \hat{W}^{\dagger}\hat{H}\hat{W}$$
$$= \hat{H}_B = \frac{(V_{12} + V_{34})}{2}\hat{I}^{(1)} \otimes \hat{\sigma}_x^{(2)} + \frac{(V_{23} + V_{14})}{2}\hat{\sigma}_z^{(1)} \otimes \hat{I}^{(2)}$$
$$+ \frac{(V_{12} - V_{34})}{2}\hat{\sigma}_x^{(1)} \otimes \hat{I}^{(2)} - \frac{(V_{23} - V_{14})}{2}\hat{I}^{(1)} \otimes \hat{\sigma}_z^{(2)}$$
$$- \frac{(V_{13} + V_{24})}{2}\hat{\sigma}_y^{(1)} \otimes \hat{I}^{(2)} + \frac{(V_{13} - V_{24})}{2}\hat{I}^{(1)} \otimes \hat{\sigma}_y^{(2)}. \qquad (6)$$

We rewrite the Hamiltonian as a linear combination of Pauli matrices $\hat{\sigma}_{(x,y,z)}$ acting separately on qubits 1 and 2, left (outer) and right (inner), respectively:

$$\hat{H}_W = \hat{h}^{(1)} \otimes \hat{I}^{(2)} + \hat{I}^{(1)} \otimes \hat{h}^{(2)}, \qquad (7a)$$
$$\hat{h}^{(1)} \equiv \text{Re}\{\Omega_{L_0}\}\hat{\sigma}_x - \text{Im}\{\Omega_{L_0}\}\hat{\sigma}_y + \Delta_L\hat{\sigma}_z, \qquad (7b)$$
$$\hat{h}^{(2)} \equiv \text{Re}\{\Omega_{R_0}\}\hat{\sigma}_x + \text{Im}\{\Omega_{R_0}\}\hat{\sigma}_y - \Delta_R\hat{\sigma}_z, \qquad (7c)$$

where

$$\Omega_{L_0} = \frac{V_{12} - V_{34}}{2} + i\frac{V_{13} + V_{24}}{2}, \Delta_L = \frac{V_{23} + V_{14}}{2}, \qquad (8a)$$
$$\Omega_{R_0} = \frac{V_{12} + V_{34}}{2} + i\frac{V_{13} - V_{24}}{2}, \Delta_R = \frac{V_{23} - V_{14}}{2}. \qquad (8b)$$

We also write the generalized Rabi frequencies of these two qubits, which is shown to be the generalization of the single Rabi frequency from the two-level case:

$$\Omega_L = \sqrt{|\Omega_{L_0}|^2 + \Delta_L^2}$$
$$= \frac{1}{2}\sqrt{|V_{12} - V_{34}|^2 + |V_{13} + V_{24}|^2 + |V_{23} + V_{14}|^2}, \qquad (9a)$$
$$\Omega_R = \sqrt{|\Omega_{R_0}|^2 + \Delta_R^2}$$
$$= \frac{1}{2}\sqrt{|V_{12} + V_{34}|^2 + |V_{13} - V_{24}|^2 + |V_{23} - V_{14}|^2}. \qquad (9b)$$

The notations presented here are summarized in Fig. 1. As illustrated from Fig. 1(a), arbitrary on-resonant real valued coefficients are allowed in the Lab frame scheme, whereas in the Bell frame scheme, shown in Fig. 1(b), the coupling coefficient between state $|\psi_1^B\rangle$ and $|\psi_2^B\rangle$ is the same as $|\psi_3^B\rangle$ and $|\psi_4^B\rangle$ (equal to Ω_{R_0}), and the coupling coefficient between state $|\psi_1^B\rangle$ and $|\psi_3^B\rangle$ is the same as for $|\psi_2^B\rangle$ and $|\psi_4^B\rangle$ (equal to Ω_{L_0}). Detunings are also allowed in the Bell frame. In both frames, the Hamiltonians contain six degrees of freedoms, which is expected from the summation of the degrees of freedom in two su(2) systems.
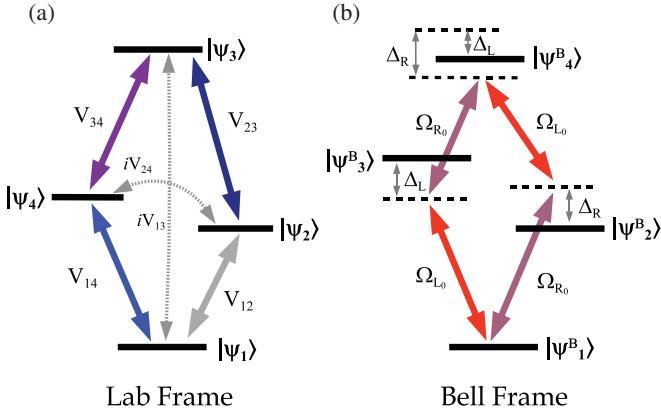
FIG. 1. (Color online) Coupling diagram of the four-mode dynamics in two different representations. (a) Lab frame representation - the couplings are real valued and can be with different values. (b) Bell frame representation—detunings are allowed and the coupling coefficients can be complex valued. Equivalence between coupling values is needed.

II. ANALYTICAL SOLUTION OF THE DYNAMICS AND GEOMETRICAL INTERPRETATION

In the language of Lie group theory, the dynamical problem factorizes into two separate problems for two SU(2) unitary operators acting on two qubits. Therefore, geometric tools for visualization of resulting solutions are readily available. By using an algebraic property of local transformations, we can represent the action of an $SU(2) \times SU(2)/Z_2$ operator on a four-dimensional state vector as left and right multiplication by two 2×2 su(2) matrices acting on a 2×2 complex matrix [20,21]. Thus we rewrite the equations for the evolution of amplitudes $a_n(t)$ of the states $|\psi_n\rangle$, $n \in \{1,2,3,4\}$ using the following rearrangement:

$$\hat{A}(t) = a_1(t)\hat{I} + a_2(t)\hat{\sigma}_x + a_3(t)i\hat{\sigma}_y + a_4(t)\hat{\sigma}_z. \quad (10)$$

Here $\hat{A}(t)$ is a two-dimensional matrix which contains the information about four amplitudes $a_n(t)$. For completeness, we write it explicitly:

$$\hat{A}(t) = \begin{pmatrix} c_1(t) & c_2(t) \\ c_3(t) & c_4(t) \end{pmatrix} = \begin{pmatrix} a_1(t) + a_4(t) & a_2(t) + a_3(t) \\ a_2(t) - a_3(t) & a_1(t) - a_4(t) \end{pmatrix}. \quad (11)$$

The general time-dependent evolution can be found in a form of two rotations of $\hat{A}(t)$, where one acts from the left u_L and the second acts from the right u_R. This can be written as

$$\hat{A}(t) = \hat{u}_L^T(t - t_0)\hat{A}(t_0)\hat{u}_R(t - t_0), \quad (12)$$

where the operators

$$\hat{u}_L(t) = \exp\left\{ i\frac{t}{2}[(V_{12} - V_{34})\hat{\sigma}_x - (V_{13} + V_{24})\hat{\sigma}_y + (V_{23} + V_{14})\hat{\sigma}_z]\right\}$$

$$= \begin{pmatrix} \cos(\Omega_L t) + i\frac{\Delta_L}{\Omega_L}\sin(\Omega_L t) & i\frac{\Omega_{L_0}^*}{\Omega_L}\sin(\Omega_L t) \\ i\frac{\Omega_{L_0}}{\Omega_L}\sin(\Omega_L t) & \cos(\Omega_L t) - i\frac{\Delta_L}{\Omega_L}\sin(\Omega_L t) \end{pmatrix},$$

$$\hat{u}_R(t) = \exp\left\{ i\frac{t}{2}[(V_{12} + V_{34})\hat{\sigma}_x + (V_{13} - V_{24})\hat{\sigma}_y - (V_{23} - V_{14})\hat{\sigma}_z]\right\}$$

$$= \begin{pmatrix} \cos(\Omega_R t) - i\frac{\Delta_R}{\Omega_R}\sin(\Omega_R t) & i\frac{\Omega_{R_0}}{\Omega_R}\sin(\Omega_R t) \\ i\frac{\Omega_{R_0}^*}{\Omega_R}\sin(\Omega_R t) & \cos(\Omega_R t) + i\frac{\Delta_R}{\Omega_R}\sin(\Omega_R t) \end{pmatrix},$$

are the local rotations of qubits 1 and 2, correspondingly. Equation (12), is an important expression which allow a simplified way to solve analytically the four mode dynamics, using multiplication of three 2 by 2 matrices.

The above dynamics can also be visualized on two separate Bloch spheres. Let us define the associated state vectors, $\vec{r}_L = (U_L, V_L, W_L)$ and $\vec{r}_R = (U_R, V_R, W_R)$, written as follows:

$$W_L = |c_1|^2 - |c_2|^2 + |c_3|^2 - |c_4|^2, \quad (13a)$$

$$U_L = c_1^*c_2 + c_1c_2^* + c_3^*c_4 + c_3c_4^*, \quad (13b)$$

$$V_L = i(c_1^*c_2 - c_1c_2^* + c_3^*c_4 - c_3c_4^*), \quad (13c)$$

and

$$W_R = |c_1|^2 - |c_3|^2 + |c_2|^2 - |c_4|^2, \quad (14a)$$

$$U_R = c_1^*c_3 + c_1c_3^* + c_2^*c_4 + c_2c_4^*, \quad (14b)$$

$$V_R = i(c_1^*c_3 - c_1c_3^* + c_2^*c_4 - c_2c_4^*). \quad (14c)$$

Here the $c_n(t)$ are the probability amplitudes in the Bell basis frame [written explicitly in Eq. (11)]. In such a basis, the dynamics can be written as two independent torque equations,

$$\frac{\partial}{\partial t}\vec{r}_L = \vec{\Omega}_L \times \vec{r}_L, \quad (15a)$$

$$\frac{\partial}{\partial t}\vec{r}_R = \vec{\Omega}_R \times \vec{r}_R, \quad (15b)$$

where $\vec{\Omega}_L = [\text{Re}\{\Omega_{L0}\}, \text{Im}\{\Omega_{L0}\}, \Delta_L]$ and $\vec{\Omega}_R = [\text{Re}\{\Omega_{R0}\}, \text{Im}\{\Omega_{R0}\}, \Delta_R]$ are their associate torque vectors. This geometrical visualization offers an intuitive physical understanding of such four-state dynamics, in the same way as for the two-level case.

III. NEAREST-NEIGHBOR COUPLINGS

In the case of periodic nearest-state coupling, where $V_{13} = V_{24} = 0$ in the Hamiltonian presented in Eq. (2), there is another symmetry which allows us to solve the problem in an elegant geometric fashion. Suppose that we choose to rotate the basis in the space spanned by vectors $|\psi_2\rangle$ and $|\psi_4\rangle$. Such a rotation apparently has no effect on the evolution of the states $|\psi_1\rangle$ and $|\psi_3\rangle$. We can represent this transformation as a phase multiplication acting on two complex vectors $(V_{12} + i V_{14}) \rightarrow (V_{12} + i V_{14}) e^{i\theta}$ and $(V_{23} + i V_{34}) \rightarrow (V_{23} + i V_{34}) e^{i\theta}$. The invariance of the amplitudes $a_1(t)$ and $a_3(t)$ under such a transformation means that the amplitudes a_1 and a_3 are determined not by the full set of coupling coefficients $\{V_{12}, V_{23}, V_{34}, V_{14}\} \in R^4$, but by an element of the quotient space $R^2 \times R^2/SO(2)$, described by a special algebraic transformation known as the Hopf $S^3 \rightarrow S^2$ projective map [22,23]. In physics, the Hopf map is commonly associated with the Bloch sphere representation of a pure state. In our problem, the map takes the four-dimensional V_{ij} space to a three-dimensional ξ_n space,

$$\xi_0 = \tfrac{1}{2}\left(V_{12}^2 + V_{14}^2 + V_{23}^2 + V_{34}^2\right), \quad (16a)$$

$$\xi_1 = V_{12}V_{23} + V_{14}V_{34}, \quad (16b)$$

$$\xi_2 = V_{12}V_{34} - V_{23}V_{14}, \quad (16c)$$

$$\xi_3 = \tfrac{1}{2}\left(V_{12}^2 + V_{14}^2 - V_{23}^2 - V_{34}^2\right). \quad (16d)$$

The new coordinates ξ_n satisfy the equation $\xi_0^2 - \xi_1^2 - \xi_2^2 - \xi_3^2 = 0$, which is the equation for a three-dimensional cone embedded in four-dimensional Euclidian space [24]. By using the projective coordinates $\{\xi_1, \xi_2, \xi_3\}$, the algebraic expressions for the amplitudes $a_n(t)$ can be significantly compacted.

As an example of the analytical solution, we find the general evolution of the states when the system is initialized in the ground state $|\psi_1\rangle$ so that $a_1(0) = 1$ and $a_{2,3,4}(0) = 0$ (in this case $\hat{A}(0) = \hat{I}$). The time-dependent amplitudes of the states $|\psi_n\rangle$ can be followed from Eq. (12),

$$a_1(t) = \cos(\Omega_L t)\cos(\Omega_R t) - \frac{\xi_3}{\sqrt{\xi_1^2 + \xi_3^2}}\sin(\Omega_L t)\sin(\Omega_R t),$$
$$(17a)$$

$$a_2(t) = i\frac{\Omega_{R0}}{\Omega_R}\cos(\Omega_L t)\sin(\Omega_R t) - i\frac{\Omega_{L0}}{\Omega_L}\sin(\Omega_L t)\cos(\Omega_R t),$$
$$(17b)$$

$$a_3(t) = -\frac{\xi_1}{\sqrt{\xi_1^2 + \xi_3^2}}\sin(\Omega_L t)\sin(\Omega_R t), \quad (17c)$$

$$a_4(t) = i\frac{\Delta_R}{\Omega_R}\cos(\Omega_L t)\sin(\Omega_R t) - i\frac{\Delta_L}{\Omega_L}\sin(\Omega_L t)\cos(\Omega_R t).$$
$$(17d)$$

It immediately follows from these relations that, the amplitudes of $a_{1,3}(t)$ remain real valued while the amplitudes of $a_{2,4}(t)$ are purely imaginary. If we look only on the solutions of $a_1(t)$ and $a_3(t)$, we can see that the structure of the solution of the four-coupled modes dynamics is the same as for the two-coupled mode one, where instead of a single Rabi frequency there are two distinct ones. This is summarized in Table I.

IV. THE PYTHAGOREAN INVERSION SCHEME

Now we have all the necessary equations to solve the problem of complete population transfer from state $|\psi_1\rangle$ to state $|\psi_3\rangle$ at time $t = \tau$, i.e.,

$$a_3(\tau) = 1, \quad a_1(\tau) = a_2(\tau) = a_4(\tau) = 0. \quad (18)$$

To do so, the requirement of on-resonant interaction should be satisfied, i.e., the ξ_3 variable, the analogue of the detuning Δ in the two-mode case, should be equal to zero. Next, complete population transfer will occur only when dynamic angles $\Omega_L t$ and $\Omega_R t$ simultaneously complete a π-phase rotation, i.e., when $\Omega_L = \frac{\pi}{2\tau}(2m_1 + 1) \equiv \frac{\pi}{2\tau}p$ and $\Omega_R = \frac{\pi}{2\tau}(2m_2 + 1) \equiv \frac{\pi}{2\tau}q$, where we defined m_1 and m_2 to be arbitrary integer numbers, and the p and q parameters are then two odd numbers. After some algebra, we derive the following solution for complete population transfer, where

$$(\xi_0, \xi_1, \xi_2) = \frac{\pi^2}{2\tau^2}\left(\frac{p^2 + q^2}{2}, pq, \frac{p^2 - q^2}{2}\right) \equiv \frac{\Omega_{\text{Pyth}}^2}{2}(c, b, a).$$
$$(19)$$

This solution exactly matches the generating function of primitive Pythagorean triples (PPTs) [25], which states that for any pair (p, q) of positive odd integers with $p > q$, the

TABLE I. Comparison of the Rabi solution for a two-mode system (the middle column) with a four-mode nearest-neighbor solution (the right column). We observe a striking similarity in the structure of both solutions.

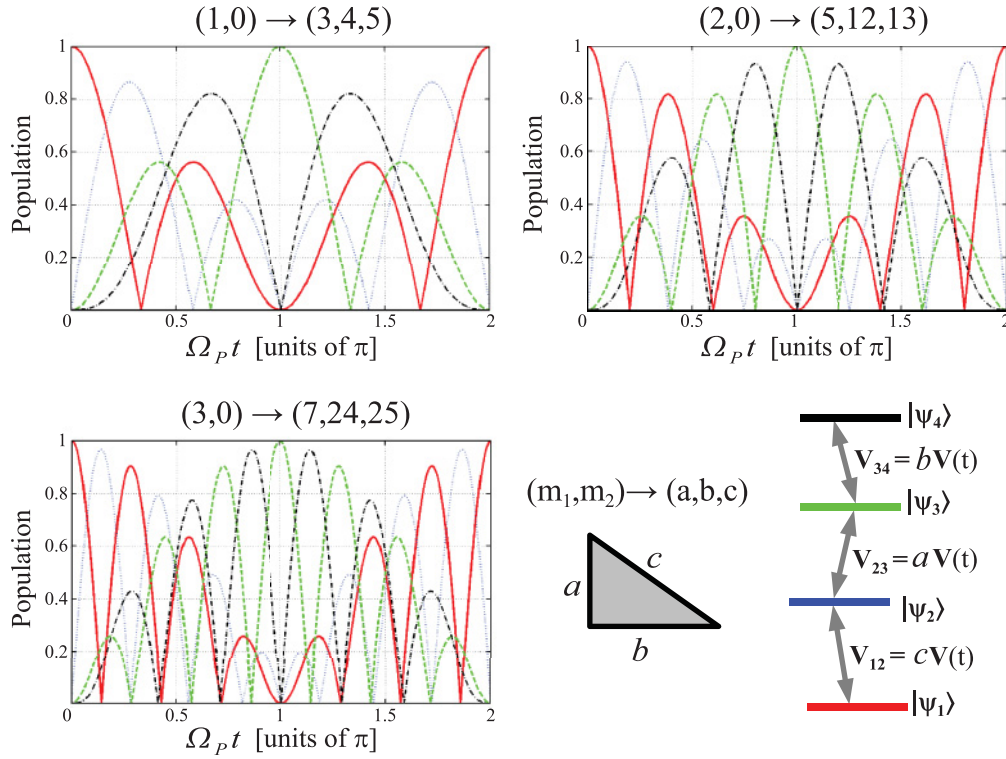| Parameter	Two-mode dynamics	Nearest-neighbor four-mode dynamics
Dynamical symmetry	SU(2)	SU(2) × SU(2)
Spanned space	$\{|\psi_g\rangle, |\psi_e\rangle\}$	$\{|\psi_1\rangle, |\psi_3\rangle\}$ and $\{|\psi_2\rangle, |\psi_4\rangle\}$
Generalized frequencies	$\Omega = \sqrt{V_{ge}^2 + \Delta^2}$	$\Omega_L = \sqrt{\Omega_{L0}^2 + \Delta_L^2}$
		$\Omega_R = \sqrt{\Omega_{R0}^2 + \Delta_R^2}$
"Torque" vector	$\vec{\Omega}_{\text{Rabi}} = \left(\text{Re}\{V_{ge}\}, \text{Im}\{V_{ge}\}, \Delta\right)$	$\vec{\Omega}_{\text{Pyth}} = \frac{2}{c}\frac{1}{\sqrt{\xi_0}}(\xi_1, \xi_2, \xi_3)$
Ground-state evolution	$a_g(t) = \cos(\Omega t) - \frac{\Delta}{\sqrt{V_{ge}^2 + \Delta^2}}\sin(\Omega t)$	$a_1(t) = \cos(\Omega_L t)\cos(\Omega_R t) - \frac{\xi_3}{\sqrt{\xi_1^2 + \xi_3^2}}\sin(\Omega_L t)\sin(\Omega_R t)$
Excited-state evolution	$a_e(t) = -\frac{V_{ge}}{\sqrt{V_{ge}^2 + \Delta^2}}\sin(\Omega t)$	$a_3(t) = -\frac{\xi_1}{\sqrt{\xi_1^2 + \xi_3^2}}\sin(\Omega_L t)\sin(\Omega_R t)$
Inversion time	$\tau = \frac{\pi}{|\Omega_{\text{Rabi}}|}$	$\tau = \frac{\pi}{|\Omega_{\text{Pyth}}|}$

FIG. 2. (Color online) Complete population transfer $|\psi_1\rangle \longleftrightarrow |\psi_3\rangle$ (or $|\psi_2\rangle \longleftrightarrow |\psi_4\rangle$). (I) State normalized populations as a function of the interaction time. The system is prepared in the ground state (solid red). The population is periodically transferred to the third state (dashed green). Parameters correspond to (a) $(m_1, m_2) = (1, 0)$, (b) $(m_1, m_2) = (2, 0)$, and (c) $(m_1, m_2) = (3, 0)$. (II) The Pythagorean triple relation between the coupling coefficients in a four-state ladder system. The computed transition time for complete population transfer matches the calculated transition time from Eq. (21).

triple $(a, b, c) \equiv \left(\frac{p^2 - q^2}{2}, pq, \frac{p^2 + q^2}{2} \right)$ is a PPT. As an example, the triples $(3; 4; 5)$ and $(5; 12; 13)$ are primitive triples, whereas $(6; 8; 10)$ is not a PPT (pythagorean triple, but not primitive). Note also that in spite of the fact that a set of numbers $(1, 1, \sqrt{2})$ satisfies the Pythagorean relation, these numbers are *not* a Pythagorean triple. Other types of generating functions of PPTs can be found elsewhere [26–28]. Equation (19) states that for the nearest-neighbor four-mode coupling problem, complete population transfer between two nonadjacent states $|\psi_1\rangle$ and $|\psi_3\rangle$ (or $|\psi_2\rangle$ and $|\psi_4\rangle$) occurs if and only if the ratio of $(\xi_0 : \xi_1 : \xi_2)$ is equal to ratio of a Pythagorean triple!

The coupling coefficients $\{V_{12}, V_{23}, V_{34}, V_{14}\}$ needed in order to achieve complete population inversion can be then obtained from Eq. (19) by inverting the transformation of Eqs. (16). Though there are several ways to do it, we choose to present the following protocol which performs such a task:

(1) Choose a Pythagorean triple. Denote it (A, B, C).

(2) Choose the ratio between the couplings $k = V_{14}/V_{12}$. It is the extra degree of freedom of the dynamics (which from a geometrical point of view can be seen as the orientation phase between the two distinct Bloch spheres).

(3) The following relation will determine the coupling coefficients:

$$V_{12} = \frac{C}{\sqrt{1 + k^2}}, \quad V_{23} = \frac{B - kA}{\sqrt{1 + k^2}},$$
$$V_{34} = \frac{A + kB}{\sqrt{1 + k^2}}, \quad V_{14} = kV_{12}. \tag{20}$$

For the special case of ladder-type coupling, where $k = 0$ and thus $V_{14} = 0$, this solution becomes $\xi_0 = V_{12}^2$, $\xi_1 = V_{23}V_{12}$, $\xi_2 = V_{34}V_{12}$, which takes a simple form of a proportion $(V_{12}; V_{23}; V_{34}) \sim (C, A, B)$.

We tested our theoretical prediction by performing numerical simulations on the dynamics of a four-level ladder transition in ^{85}Rb: $5S_{1/2} \leftrightarrow 5P_{3/2} \leftrightarrow 4D_{3/2} \leftrightarrow 4F_{5/2}$, with resonant CW interaction of 780.2 nm, 1.529 μm, and 1.344 μm, respectively. The coupling coefficients were chosen to satisfy the simplest Pythagorean triple ratio $(V_{12} : V_{23} : V_{34}) \sim (C : A : B)$. As seen in Fig. 2, numerical results are in complete agreement with the analytical solution and confirm that there is periodic population transfer between states $|\psi_1\rangle$ and $|\psi_3\rangle$. The time period for complete population transfer is given by

$$\tau \equiv \frac{\pi}{\Omega_{\text{Pyth}}} = \frac{2}{C} \frac{\pi}{\sqrt{\Omega_L^2 + \Omega_R^2}} = \frac{\pi}{\sqrt{2}C}. \tag{21}$$

Here we denoted the transition time required to achieve population transfer as Ω_{Pyth}, analogous with the Rabi frequency for a two-level dynamics, where both scale as the absolute value of the torque vector.

The next step was to check the evolution of the amplitude probabilities when the value of k was varied, which is the free parameter. For the Pythagorean relation of $m_1 = 1, m_2 = 0$ (or $A = 3, B = 4, C = 5$), we present in Fig. 3 the evolution of the system in different values of k. As expected, the amplitude probabilities of $|\psi_1\rangle$ and $|\psi_3\rangle$ remain the same for any k, while the amplitude probabilities of $|\psi_2\rangle$ and $|\psi_4\rangle$ changed
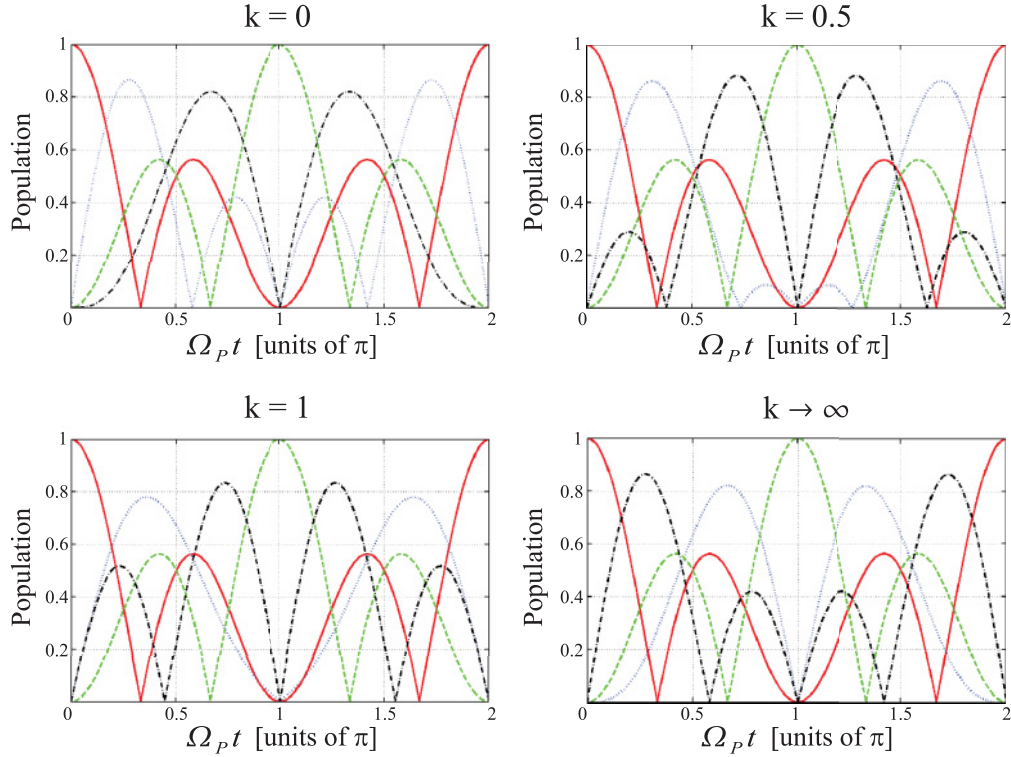
FIG. 3. (Color online) Evolution of the normalized populations with different k-values. As seen the population amplitudes of states $|\psi_1\rangle$ (solid red) and $|\psi_3\rangle$ (dashed green) remain the same for all values of k.

dramatically. This indicates again the existence of an extra phase between the two independent qubits, which does not influence the inherent dynamics of the full system, but only the projection of the evolution of one qubit from the viewpoint of the second qubit.

Another interesting question that could be raised is whether one can find the couplings that guarantee complete "switching" of information between the states of the qubits, or in mathematical terms, what will be the constraints to start with a general complex value of four probability amplitudes $a_i(0) = (\alpha, \beta, \gamma, \delta)$, which could obtain, after time τ, that *any* set of probability amplitudes will be exchanged $|\psi_1\rangle \leftrightarrow |\psi_3\rangle$ and $|\psi_2\rangle \leftrightarrow |\psi_4\rangle$, i.e., that $a_i(\tau) = (\gamma, \delta, \alpha, \beta)$. In the quantum literature this is known as a "dual-rail" mechanism.

For the case of periodic nearest-state coupling ($V_{13} = V_{24} = 0$), such constraints can be found. It requires that $k = \frac{C-B}{A}$, resulting in the following coupling coefficients:

$$V_{12} = V_{34} = B\sqrt{\frac{C}{2(C-A)}}, \tag{22a}$$

$$V_{14} = V_{23} = \sqrt{\frac{C(C-A)}{2}}. \tag{22b}$$

We again checked our prediction by choosing the Pythagorean relation of $m_1 = 1, m_2 = 0$, or $(A,B,C) = (3,4,5)$. By fixing the parameter and choosing an arbitrary complex valued wave function, we see in Fig. 4 that after an inversion time (where $\tau = \pi/\Omega_{\text{Pyth}}$), the evolution of probability amplitude of each state is "exchanged" with the value of its counterpart. From a geometrical point of view,

the dynamics of the two separate su(2)'s evolve with the same parameters of the torque vectors.

In conclusion, the dynamics of four-state systems were analyzed from a geometric perspective. We have shown that
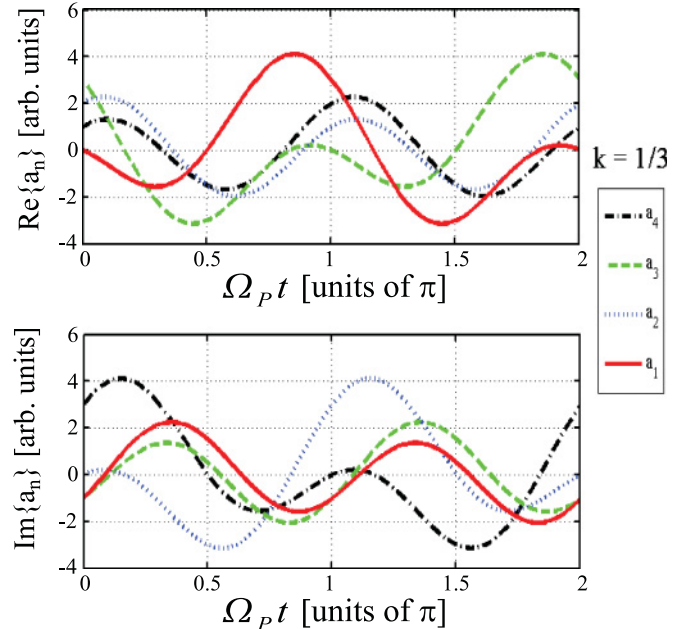

FIG. 4. (Color online) The dual-rail mechanism. As seen, the initial probability amplitudes $a_n(0) = (-i, 2, 3-i, 1+3i)$ transfer "information" between $|\psi_1\rangle \leftrightarrow |\psi_3\rangle$ and $|\psi_2\rangle \leftrightarrow |\psi_4\rangle$, after a period of $\tau = \frac{\pi}{\Omega_{\text{Pyth}}}$.

such systems can be decomposed into two separate qubits, each with its own characteristics. Two frames of the dynamics were explored, each highlighting a different aspect of the system, and a general analytical solution was written. The main focus of the article is the identification of a scheme for complete population transfer in such systems. We observed very close connection between the structure of solution for the nearest-neighbor coupling four-state system and the family of primitive Pythagorean triples. Due to its simplicity and clear geometric structure, the identified solution may be important for quantum information and quantum computing applications and as a state preparation technique for both population or entanglement transfer [6]. Though the dynamics of four-state systems were analyzed here in the realization of atomic physics, we shall note again that all the analytical results can be implemented in other physical realizations as well. Also, those results can be used for some problems of spatial propagation of light pulses, such as the coupling between directional waveguides, and multimode fibers. We expect that similar solutions, revealing a deeper link with number theory, can be found for six- and eight-state systems. The present method can also be generalized to include more complex, exactly solvable two-state models.

APPENDIX: EXPLICIT ALGEBRAIC DECOMPOSITION

For completeness, we choose here to write the explicit decomposition of the Hamiltonian in both frames. In the Lab frame it is

$$
\begin{aligned}
\hat{H} =& \frac{(V_{12}+V_{34})}{2}\begin{pmatrix} \hat{\sigma}_x & 0 \\ 0 & \hat{\sigma}_x \end{pmatrix} + \frac{(V_{23}+V_{14})}{2}\begin{pmatrix} 0 & \hat{\sigma}_x \\ \hat{\sigma}_x & 0 \end{pmatrix} + \frac{(V_{12}-V_{34})}{2}\begin{pmatrix} \hat{\sigma}_x & 0 \\ 0 & -\hat{\sigma}_x \end{pmatrix} \\
&+ \frac{(V_{23}-V_{14})}{2}\begin{pmatrix} 0 & -i\hat{\sigma}_y \\ i\hat{\sigma}_y & 0 \end{pmatrix} + \frac{i(V_{13}+V_{24})}{2}\begin{pmatrix} 0 & -\hat{I} \\ \hat{I} & 0 \end{pmatrix} + \frac{i(V_{13}-V_{24})}{2}\begin{pmatrix} 0 & -\hat{\sigma}_z \\ \hat{\sigma}_z & 0 \end{pmatrix} \\
=& \frac{(V_{12}+V_{34})}{2}\hat{I}^{(1)}\otimes\hat{\sigma}_x^{(2)} + \frac{(V_{23}+V_{14})}{2}\hat{\sigma}_x^{(1)}\otimes\hat{\sigma}_x^{(2)} + \frac{(V_{12}-V_{34})}{2}\hat{\sigma}_z^{(1)}\otimes\hat{\sigma}_x^{(2)} \\
&+ \frac{(V_{23}-V_{14})}{2}\hat{\sigma}_y^{(1)}\otimes\hat{\sigma}_y^{(2)} + \frac{(V_{13}+V_{24})}{2}\hat{\sigma}_y^{(1)}\otimes I^{(2)} + \frac{(V_{13}-V_{24})}{2}\hat{\sigma}_y^{(1)}\otimes\hat{\sigma}_z^{(2)}.
\end{aligned} \tag{A1}
$$

The explicit decomposition in the Bell frame is:

$$
\begin{aligned}
\hat{H}_B =& \hat{W}^\dagger \hat{H} \hat{W} \\
=& \frac{(V_{12}+V_{34})}{2}\begin{pmatrix} \hat{\sigma}_x & 0 \\ 0 & \hat{\sigma}_x \end{pmatrix} + \frac{(V_{23}+V_{14})}{2}\begin{pmatrix} \hat{I} & 0 \\ 0 & -\hat{I} \end{pmatrix} + \frac{(V_{12}-V_{34})}{2}\begin{pmatrix} 0 & \hat{I} \\ \hat{I} & 0 \end{pmatrix} \\
&- \frac{(V_{23}-V_{14})}{2}\begin{pmatrix} \hat{\sigma}_z & 0 \\ 0 & \hat{\sigma}_z \end{pmatrix} - \frac{i(V_{13}+V_{24})}{2}\begin{pmatrix} 0 & -\hat{I} \\ \hat{I} & 0 \end{pmatrix} + \frac{(V_{13}-V_{24})}{2}\begin{pmatrix} \hat{\sigma}_y & 0 \\ 0 & \hat{\sigma}_y \end{pmatrix} \\
=& \frac{(V_{12}+V_{34})}{2}\hat{I}^{(1)}\otimes\hat{\sigma}_x^{(2)} + \frac{(V_{23}+V_{14})}{2}\hat{\sigma}_z^{(1)}\otimes\hat{I}^{(2)} + \frac{(V_{12}-V_{34})}{2}\hat{\sigma}_x^{(1)}\otimes\hat{I}^{(2)} \\
&- \frac{(V_{23}-V_{14})}{2}\hat{I}^{(1)}\otimes\hat{\sigma}_z^{(2)} - \frac{(V_{13}+V_{24})}{2}\hat{\sigma}_y^{(1)}\otimes\hat{I}^{(2)} + \frac{(V_{13}-V_{24})}{2}\hat{I}^{(1)}\otimes\hat{\sigma}_y^{(2)}
\end{aligned} \tag{A2}
$$

[1] L. Allen, and J. H. Eberly, *Optical Resonance and Two Level Systems* (Dover, New York, 1975).

[2] J. Gong and S. A. Rice, Phys. Rev. A **69**, 063410 (2004).

[3] J. Gong and S. A. Rice, J. Chem. Phys. **120**, 9984 (2004).

[4] J. Keeler, *Understanding NMR Spectroscopy* (John Wiley and Sons, New York, 2005).

[5] M. A. Nielsen and I. L. Chuang, *Quantum Computation and Quantum Information* (Cambridge University Press, Cambridge, 2000).

[6] A. Sorensen and K. Molmer, Phys. Rev. Lett. **82**, 1971 (1999).

[7] A. Yariv, IEEE, J. Quantum Electronics **9**, 9 (1973).

[8] H. Rabitz and G. Turinici, Chem. Phys. **267**, 1 (2001).

[9] D. Tannor, *Introduction to Quantum Mechanics: A Time-dependent Perspective* (University Science Books, Herndon, VA, 2007).

[10] J. R. Kuklinski, U. Gaubatz, F. T. Hioe, and K. Bergmann, Phys. Rev. A **40**, 6741 (1989).

[11] V. S. Malinovsky and D. J. Tannor, Phys. Rev. A **56**(6), 4929 (1997).

[12] N. V. Vitanov, B. W. Shore, and K. Bergmann, Eur. Phys. J. D **4**(15), 29 (1998).

[13] Y. N. Demkov and V. I. Osherov, Sov. Phys. JETP **26**, 916 (1968).

[14] R. Cook and B. Shore, Phys. Rev. **20**, 539 (1979).

[15] B. W. Shore, K. Bergmann, A. Kuhn, S. Schiemann, J. Oreg, and J. H. Eberly, Phys. Rev. A **45**, 5297 (1992).

[16] M. Born and E. Wolf, *Principles of Optics* (Cambridge University Press, Cambridge, 1999).

[17] F. Bloch, Phys. Rev. **70**, 460 (1946).

[18] D. Uskov and A. R. P. Rau, Phys. Rev. A **78**, 022331 (2008).

[19] A. R. P. Rau, Phys. Rev. A **61**, 032301 (2000).

[20] P. Levay, J. Phys. A **38**(41), 9075 (2007).

[21] P. Du Val, *Homographies, Quaternions and Rotations* (Oxford Mathematical Monographs, 1964).

[22] H. Hopf, Math. Ann. **104**, 637 (1931).

[23] D. W. Lyons, Math. Mag. **76**(2), 87 (2003).

[24] J. Kocik, Adv. Appl. Clifford Algebras **17**(1), 71 (2006).

[25] [http://aleph0.clarku.edu/djoyce/java/elements/elements.html] (2007).

[26] F. J. M. Barning, Math. Centrum Amsterdam Afd. Zuivere Wisk **ZW-011**, 37 (1963).

[27] P. J. Arpaia, Math. Mag. **44**, 26 (1971).

[28] D. McCullough and E. Wade, College Math. J. **34**, 107 (2003).